

A model for a flywheel automatic assisted manual transmission

Original

A model for a flywheel automatic assisted manual transmission / Galvagno, Enrico; Velardocchia, Mauro; Vigliani, Alessandro. - In: MECHANISM AND MACHINE THEORY. - ISSN 0094-114X. - 44:(2009), pp. 1294-1305.
[10.1016/j.mechmachtheory.2008.07.002]

Availability:

This version is available at: 11583/1797715 since:

Publisher:

Published

DOI:10.1016/j.mechmachtheory.2008.07.002

Terms of use:

This article is made available under terms and conditions as specified in the corresponding bibliographic description in the repository

Publisher copyright

(Article begins on next page)

A model for a flywheel assisted automated manual transmission

E. Galvagno, M. Velardocchia, A. Vigliani

Dipartimento di Meccanica - Politecnico di Torino
C.so Duca degli Abruzzi, 24 - 10129 Torino - ITALY
E-mail: alessandro.vigliani@polito.it

Keywords automated manual transmissions, flywheel, automotive transmissions, torque gap filler

Abstract *This paper is focused on the model and dynamical analysis of a flywheel assisted transmission aiming at reducing the torque gap during gear shift manoeuvres. This completely passive device, consisting of a planetary gear set mounting a flywheel on the sun gear shaft, allows to continuously connect the engine to the load shaft. Depending on the operating conditions, it can either absorb energy from the engine or deliver the previously stored kinetic energy to the wheels when the clutch is disengaged, thus allowing better vehicle performances and/or ride comfort through a suitable coordinated control of engine and clutch.*

1 Introduction

The study of automotive transmissions has been faced up deeply during last years, with the aim of obtaining better vehicle performances, in particular during the gear shift phase and, eventually, to reduce the fuel consumption [Kulkarni et al. (2007); Serrarens et al. (2003); Koprubasi et al. (2007)]. Among this general background, depending on the transmission type, different problems still require to be solved: torque gap for manual transmission (MT)[Kuroiwa et al. (2004); Sornioti et al. (2007)]; engine rotating inertia acceleration for continuously variable transmission (CVT)[Vroemen et al. (2004)]; efficiency for automatic transmission (AT) [Park et al. (2000)].

To reduce such drawbacks, many car makers recently started to develop new systems. Torque gap fillers (TGF) devices can be used on automated manual transmissions (AMT) aiming at eliminating or at least reducing the torque gap that occurs during gear shifting transients [Kuroiwa et al. (2004)]. Dual-clutch transmission (DCT) realize shifts by torque transfer from one clutch to another without traction interruption due to the controlled slippage of the clutches [Kulkarni et al. (2007)]. Other solutions are represented by CVT equipped with power splitting epicyclic gears mounting a steel flywheel in the so-called zero inertia (ZI) powertrain [van Druten (2001)]. The impulse shift (IS) principle was introduced ([Vroemen et al. (2004)]) to improve ZI systems, allowing reduced flywheels size and further improving the vehicle response during transients.

All these systems aim at two opposite goals: enhancing the vehicle driveability in terms of accelerator response and optimizing the fuel consumption. To achieve these results, it is necessary to drive the vehicle at low engine velocities in steady state manoeuvres; in case a power splitting device is adopted, energy stored in the flywheel can be delivered to the wheels during the gear shifts transients. The energy may be accumulated during the accelerator back-out phase or during the acceleration phase with fixed gear [Serrarens et al. (2003)].

In this paper the authors present the model of a driveline to be used in vehicles equipped with AMT; the classical layout is modified with an additional epicyclic gearing mounted between the engine shaft and the gearbox output shaft, connected also with a flywheel. The purpose of this additional equipment is to reduce the torque gap occurring during the gear shifts by means of a completely passive device; this result can be achieved bypassing the gearbox during the transitory of up or down shifts. A suitable coordinated control of engine and clutch is necessary to optimize the system performances. It is worth to underline that the presence of such devices should not cause significant losses during the normal vehicle run.

2 Driveline model

The proposed driveline (Fig. 1), with a flywheel mounted on the sun gear of an epicyclic train to be positioned between the engine shaft (linked to the ring) and the gearbox output shaft (connected to the carrier), shows a different dynamic behaviour depending on the clutch status; hence three scenarios are possible:

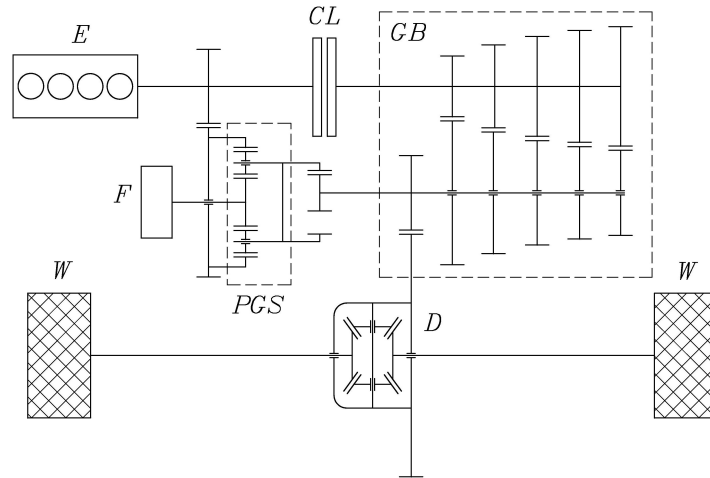


Figure 1: Sketch of the proposed driveline

- clutch in sliding conditions, gear engaged: the system has two d.o.f. and the speed ratio $i = \omega_e/\omega_l$ between the engine and secondary shafts is not constant;
- clutch disengaged, down shift or up shift phase: the gearbox is bypassed, the system has two d.o.f. since the synchronization dynamics is neglected and the speed ratio i is not constant;
- clutch engaged, gear engaged: the speed ratio i is constant and the system possesses a single degree of freedom.

In the following subsections, after the model of the epicyclic gear train, the three different situations, with the correspondent dynamic equations, will be analysed.

The one d.o.f. vehicle dynamics is modelled with an equivalent inertia (J_l) and torque (T_l) acting on secondary shaft, i.e.:

$$J_l = \frac{mR^2 + 4J_w}{\tau_f^2} \quad \text{and} \quad T_l = \frac{[F_0 + F_2 V^2 + mg \sin(\arctan \delta)] R}{\tau_f}, \quad (1)$$

where m is the vehicle mass, R is the wheel radius, J_w is the wheel inertia, τ_f is the final reduction, V is the vehicle speed, F_0 and F_2 are the experimental coast-down coefficients of the vehicle and δ is the road slope.

2.1 Model of the epicyclic gear train

The classical epicyclic gearing is shown in Fig. 2, where also the sign conventions for the angular speeds and torques are visible. This mechanism has two d.o.f., so the velocity of the sun can be evaluated from the carrier and ring speeds:

$$\omega_s = (1 + \sigma) \omega_c - \sigma \omega_r, \quad (2)$$

where $\sigma = R_r/R_s$ is the ratio between the radii of ring and sun gears.

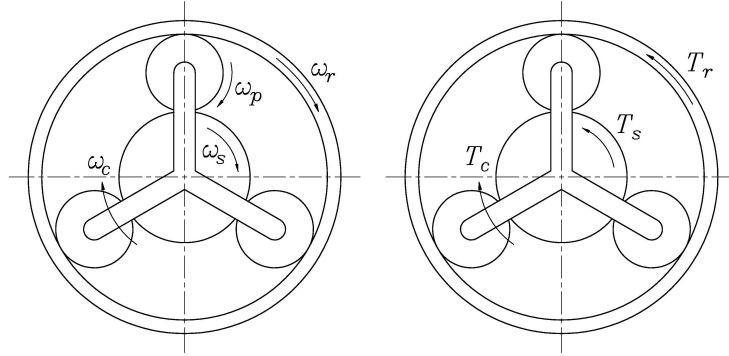


Figure 2: Epicyclic gear train: velocities (left) and torques (right)

It is convenient to define also the ratio $\bar{i} = (1 + \sigma)/\sigma$, which represents the particular speed ratio between the ring and the carrier correspondent to a null velocity of the sun ($\omega_s = 0$); obviously it follows that if $\omega_r/\omega_c > \bar{i}$ then $\omega_s < 0$ and vice versa.

In order to outline the contribution of the inertia mounted on the sun, in what follows the inertias of the gears of the epicyclic train will be neglected (i.e. $J_i = 0, \forall i$); moreover, for the sake of simplicity, also the losses due to friction and meshing will not be considered (i.e. $\eta = 1$).

Hence it yields:

$$\frac{T_r}{T_s} = \sigma \quad (3)$$

and

$$\frac{T_c}{T_s} = 1 + \sigma. \quad (4)$$

2.2 Clutch in sliding conditions and gear engaged

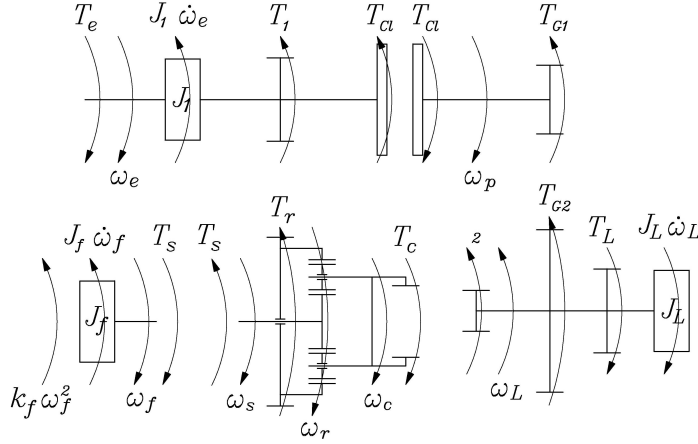


Figure 3: Free body diagrams when the clutch is sliding and a gear is engaged

When the clutch is sliding and the gear engaged (Fig. 3) the ratio $i = \omega_e/\omega_l$ is not constant and the primary shaft speed ω_p is imposed by the kinematics of the selected gearbox ratio τ : $\omega_p = \tau\omega_l$.

Let $i_1 = |\omega_e/\omega_r|$ and $i_2 = |\omega_c/\omega_l|$ be the velocity ratios respectively between the engine and the ring and between the carrier and the output shaft; with reference to the sign conventions of Figures 3 and 4, it holds:

$$\omega_e = -i_1\omega_r \quad \text{and} \quad \omega_l = -\frac{\omega_c}{i_2} \quad (5)$$

Since the flywheel is connected to the sun gear ($\omega_f = \omega_s$) of the planetary gear train, from Eq.(2) it holds:

$$\omega_f = \frac{\sigma}{i_1}\omega_e - i_2(1 + \sigma)\omega_l = \alpha_p\omega_e - \alpha_s\omega_l, \quad (6)$$

where

$$\alpha_p = \frac{\sigma}{i_1} \quad \text{and} \quad \alpha_s = i_2(1 + \sigma). \quad (7)$$

Let $i^* = \alpha_s/\alpha_p$ represent the particular speed ratio between the engine and the secondary shaft that annihilates the flywheel speed; therefore Eq.(6) can be expressed as:

$$\omega_f = \alpha_p\omega_e \left(1 - \frac{i^*}{i}\right) = \alpha_p\omega_l (i - i^*). \quad (8)$$

Consequently, since ω_e and ω_l are always positive in forward driving, it yields:

$$\begin{cases} \omega_f > 0 & \text{if } i > i^* \\ \omega_f < 0 & \text{if } i < i^* \end{cases} \quad (9)$$

Equation (6) can be derived to obtain the relationship between angular accelerations:

$$\dot{\omega}_f = \alpha_p\dot{\omega}_e - \alpha_s\dot{\omega}_l. \quad (10)$$

The following equations hold for the engine and load shafts respectively:

$$T_e - J_1\dot{\omega}_e - \frac{T_r}{i_1} - T_{cl} = 0 \quad (11)$$

$$T_l + J_l\dot{\omega}_l - i_2T_c - T_{G2} = 0, \quad (12)$$

where T_{cl} is the torque transmitted by the clutch in sliding conditions and T_{G2} is the torque exerted by the gearbox primary shaft on the output shaft. Subscript $_e$ refers to the engine, $_l$ to the secondary shaft, $_r$ to the ring, $_s$ to the sun, $_c$ to the carrier and $_cl$ to the clutch.

Obviously, it holds:

$$T_{G2} = \tau T_{cl}, \quad (13)$$

where τ is the gearbox ratio (i.e. $\tau = \omega_p/\omega_l$).

Remembering that the sun gear is connected to the flywheel, under the hypothesis that the power losses are due to air drag effect, it yields:

$$T_s = J_f \dot{\omega}_f + k_f \omega_f^2 \text{sign } \omega_f \quad (14)$$

where k_f is the constant accounting for the power losses.

From the equilibrium equations of the planetary gear train (3) and (4), it holds:

$$T_r = \sigma J_f \dot{\omega}_f + \sigma k_f \omega_f^2 \text{sign } \omega_f \quad (15)$$

and

$$T_c = (1 + \sigma) J_f \dot{\omega}_f + (1 + \sigma) k_f \omega_f^2 \text{sign } \omega_f. \quad (16)$$

Since

$$T_1 = \frac{T_r}{i_1} \quad \text{and} \quad T_2 = T_c i_2 \quad (17)$$

and introducing

$$\beta_p = \frac{\alpha_p^2 J_f}{J_l + \alpha_s^2 J_f} i^* \quad \text{and} \quad \beta_s = \frac{\alpha_p^2 J_f}{J_1 + \alpha_p^2 J_f} i^*, \quad (18)$$

after a few passages, it yields:

$$\begin{aligned} T_e - \beta_p T_l + (\tau \beta_p - 1) T_{cl} - [J_1 + \alpha_p^2 (1 - i^* \beta_p) J_f] \dot{\omega}_e + \\ - \alpha_p^3 k_f (1 - i^* \beta_p) \left(1 - \frac{\omega_l}{\omega_e} i^*\right)^2 \omega_e^2 \text{sign} \left(1 - \frac{\omega_l}{\omega_e} i^*\right) = 0 \end{aligned} \quad (19)$$

$$\begin{aligned} \beta_s T_e - T_l + (\tau - \beta_s) T_{cl} - [J_l + \alpha_p^2 i^* (i^* - \beta_s) J_f] \dot{\omega}_l + \\ + \alpha_p^3 k_f (i^* - \beta_s) \left(i^* - \frac{\omega_e}{\omega_l}\right)^2 \omega_l^2 \text{sign} \left(1 - \frac{\omega_l}{\omega_e} i^*\right) = 0. \end{aligned} \quad (20)$$

The power flows from the engine to the wheels along two different paths, i.e. through gearbox and planetary gear set; the power splits according to the difference between the engine and clutch torques. It is worth noting that, since $1 - i^* \beta_p \geq 0$ and $i^* - \beta_s \geq 0$, then the additional inertial term multiplying J_f is always positive both on the engine and on the load shaft.

Moreover the flywheel losses have a driven effect on the secondary shaft if $\omega_f > 0$, i.e. $i > i^*$; an opposite behaviour takes place on the engine shaft. Such effect can be explained considering that when $\omega_f > 0$ the air drag torque, that is always resistant on the flywheel shaft, has the same sign of the inertial torque (opposite to the flywheel acceleration) when $\dot{\omega}_f > 0$, thus increasing the reaction torque exerted on the sun shaft; consequently also the torque transmitted to the wheels is increased.

2.3 Clutch disengaged and gear shift

The case in which the clutch is open corresponds to a particular condition of the sliding situation: in fact the torque transmitted by the clutch is null (i.e. $T_{cl} = 0$), but the driveline still possesses two d.o.f. and the ratio i is not constant. Since no torque acts on the primary shaft, the synchronization phase can be actuated exactly like a MT without modifying the design of the internal components of a traditional gearbox. The synchronization dynamics can be neglected, so the gear shift will be modelled simply by imposing a step change of the ratio between the primary and the secondary shaft speeds.

Under these circumstances, all the engine energy flows through the planetary gear set, while the reaction torque needed to transmit power to the wheels is delivered by the inertial effect of the flywheel and, depending on the sign of ω_f , by its spin losses.

2.4 Clutch engaged and gear engaged

During the normal driveline operation, the ratio $i = \omega_e/\omega_l$ is equal to the ratio between the velocities of the primary and secondary shaft since it is imposed by the selected gear; hence it is constant ($i = \tau$).

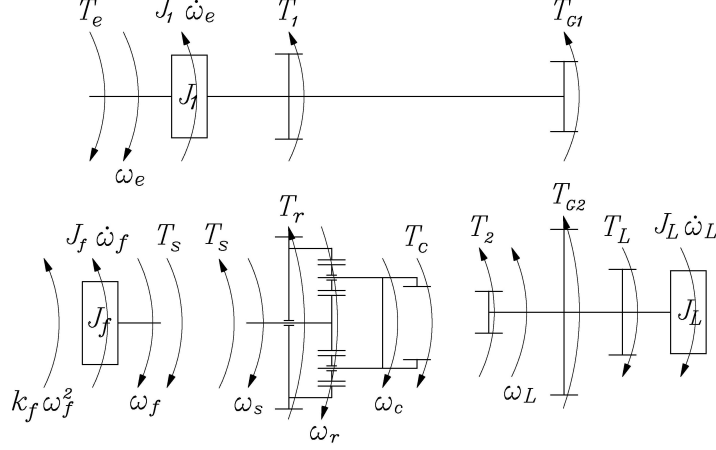


Figure 4: Force diagrams when the clutch is engaged

When the clutch is closed and a gear is engaged (Fig. 4), the engine and load shaft equilibrium equations become respectively:

$$T_e - J_1 \dot{\omega}_e - \frac{T_r}{i_1} - T_{G1} = 0 \quad (21)$$

$$T_l + J_l \dot{\omega}_l - i_2 T_c - T_{G2} = 0, \quad (22)$$

while

$$T_{G1} = \frac{T_{G2}}{\tau} \quad (23)$$

and, being i constant,

$$\dot{\omega}_e = \tau \dot{\omega}_l; \quad (24)$$

the flywheel acceleration is:

$$\dot{\omega}_f = \alpha_p (\tau - i^*) \dot{\omega}_l. \quad (25)$$

It is evident that the system has now only one d.o.f. described by the following equation:

$$T_e \tau - T_l - \left[J_1 \tau^2 + J_l + \alpha_p^2 (\tau - i^*)^2 J_f \right] \dot{\omega}_l - \alpha_p^3 k_f |\tau - i^*|^3 \omega_l^2 = 0. \quad (26)$$

It must be noted that both additional flywheel inertia and spin losses have always a resistant effect on the system acceleration with fixed gear, their importance growing with the difference between the gear ratio τ and the ratio i^* . In stationary conditions (i.e. $\dot{\omega}_l = 0$), part of the engine power must flow through the sun in order to sustain the flywheel constant rotation.

3 FAT dynamic behaviour

The following situations can be observed (Fig.5):

- **constant speed with fixed gear:** under the hypothesis of negligible rotor losses ($k_f = 0$), the power supplied by the engine is completely transferred into the driveline through the clutch, while both the input and output powers of the epicyclic gear are null (a);

- **acceleration with fixed gear:** the power supplied by the engine flows both into the gear-box through the clutch and into the epicyclic train. This operating condition is always unfavourable for the vehicle acceleration (b);
- **gear shift with clutch disengaged:** the power supplied by the engine is completely transferred to the epicyclic gear. Depending on the value of i and on the sign of $\dot{\omega}_f$ two opposite situations occur:
 - when $i < i^*$ and $\dot{\omega}_f < 0$ or $i > i^*$ and $\dot{\omega}_f > 0$, the power transmitted to the wheels is smaller than the engine power, since part of the available energy is stored in the flywheel (c);
 - when $i > i^*$ and $\dot{\omega}_f < 0$ or $i < i^*$ and $\dot{\omega}_f > 0$, the engine power is amplified, since the flywheel supplies energy to the load shaft (d).

However, both these conditions guarantee a continuous mechanical link between engine and load shafts also when the clutch is open, hence increasing the total power available at the wheels.

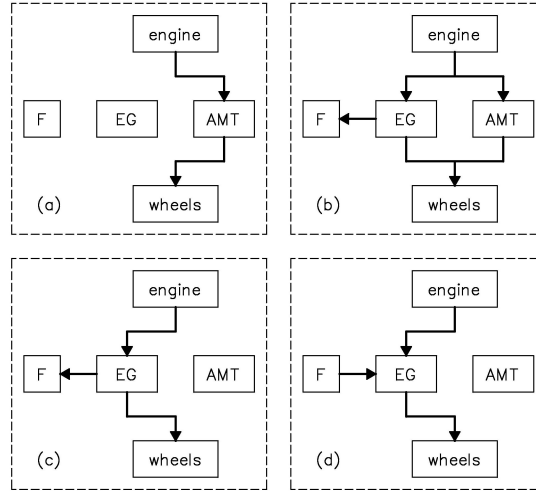


Figure 5: Different power flows: constant speed (a); acceleration (b); gear shift (c) and (d).

It is interesting to observe that, neglecting the flywheel losses (i.e. $k_f = 0$), when the clutch is disengaged eq. (20) reduces to

$$T_e \beta_s - T_l - [J_l + \alpha_p^2 i^* (i^* - \beta_s) J_f] \dot{\omega}_l = 0; \quad (27)$$

hence the engine equivalent torque acting on the load shaft is equal to the engine torque multiplied by the coefficient β_s (see Fig. 6): this coefficient is null when no flywheel is present (i.e. $J_f = 0$), while it tends to i^* for large flywheels ($J_f \rightarrow \infty$).

Similarly, but with opposite effects on the dynamics, the additional inertial term due to the flywheel $\alpha_p^2 i^* (i^* - \beta_s) J_f$ is null when $J_f = 0$ while it tends to $i^{*2} J_1$ for $J_f \rightarrow \infty$.

Since β_s is always smaller than i^* , it is possible to prove that the equivalent inertia at the secondary shaft is always larger than the correspondent equivalent inertia of the same system with an ordinary gearing having a ratio β_s (i.e. $\beta_s^2 J_1$). It is not so obvious that an increase of the flywheel size reduces the equivalent inertia in comparison with an ordinary gear, up to reaching the same value for $J_f \rightarrow \infty$; in this limit condition the sun is blocked and so the planetary gear train behaves exactly like an ordinary gearing with ratio i^* ; hence the speed ratio tends to the torque ratio.

Fig. 6 plots β_s versus the flywheel inertia J_f : an increase of inertia has initially a strong effect on the dynamics, while its influence becomes negligible for higher values. The figure also plots the various ratios τ of the gearbox and the ratio i^* , whose choice is evidently a fundamental design parameter.

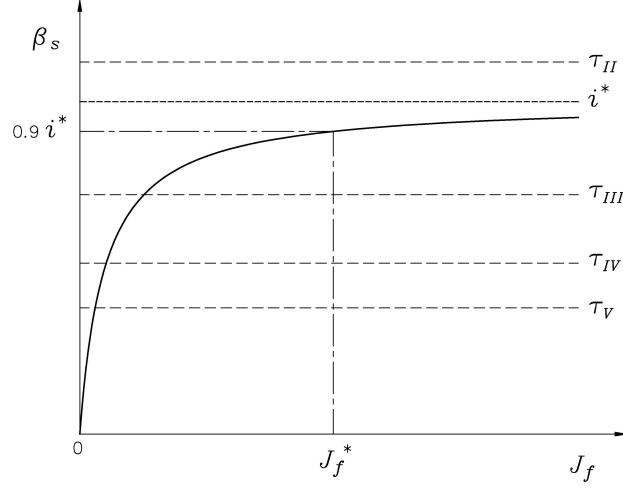


Figure 6: Torque multiplying parameter β_s versus flywheel inertia ($J_f^* = 9J_1/\alpha_p^2$)

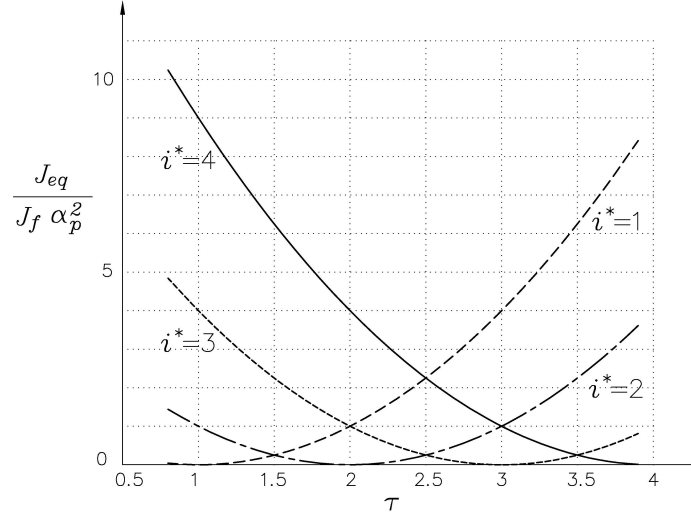


Figure 7: Flywheel non dimensional equivalent inertia $\tilde{J}_{eq} = (\tau - i^*)^2$ on the secondary shaft versus gearbox ratio at fixed gear for various i^*

Let $\gamma = \beta_s/i^*$; then an appropriate choice of γ allows to compute the flywheel inertia \bar{J}_f

$$\bar{J}_f = \frac{\gamma J_1}{(1 - \gamma)\alpha_p^2} \quad (28)$$

that represents a compromise between the advantages of the torque amplifying effect during a gear shift (Fig. 6) and the drawbacks due to additional inertia during acceleration at constant gear (Fig. 7).

Moreover the presence of the flywheel has a positive effect during the gear shift transients, for it provides energy to the driven shaft when a manual transmission does not. Conversely, when the clutch is engaged, the equivalent flywheel inertia on the load shaft causes an increase of the total inertia and therefore a decrease of the vehicle acceleration, unless $\tau = i^*$.

A compromise is necessary in order to optimize the performances during the gear shift phases and the accelerations with gear engaged: with reference to Fig. 7, it seems convenient to choose the value of i^* inside the gearbox ratios.

In Fig. 8 the ratio between the load shaft power $P_l = \beta_s T_e \omega_l$ and the engine power $P_e = T_e \omega_e$ during a gear shift is plotted versus i : $P_l/P_e = \beta_s/i$. The four regions identified in the figure represent the different power flows from the engine to the wheels when the clutch is open and are also sketched in case (c) and case (d) of Fig. 5. The flywheel absorbs energy in case (c)

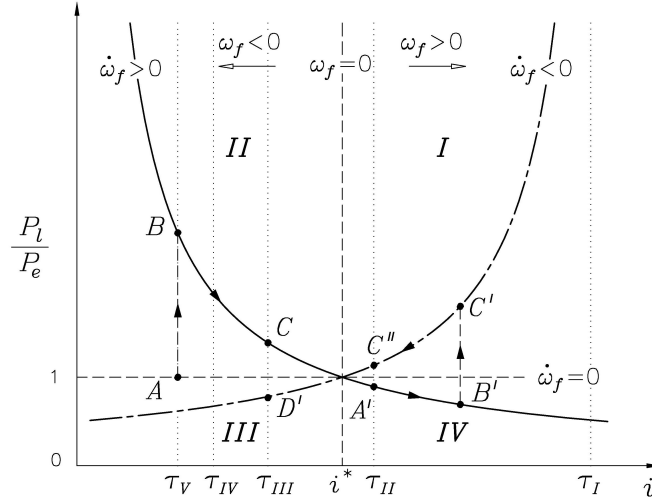


Figure 8: Ratio between the power transferred to the load shaft and the power delivered by the engine versus i during a gear shift for two different constant flywheel accelerations

corresponding to regions *III* and *IV*, when it increases the modulus of its speed, while it releases stored energy in case (d), corresponding to regions *I* and *II*.

3.1 Down shift

Let now analyse a down shift phase in detail (see Fig.8): starting from an energy efficient point *A* of the engine map (i.e. high load and low speed) in steady-state conditions, with the highest available gear engaged (τ_V), the torque reserve to accelerate the vehicle is evidently very low; hence the accelerator to wheel response is very weak. However, when the clutch is open, the engine can continue to deliver its torque, thus accelerating its shaft and consequently the load shaft (i.e. the vehicle) with a torque ratio β_s ; in the meanwhile the flywheel accelerates from a negative velocity, thus delivering part of its kinetic energy to the load shaft. These two effects together increase the total power at the wheels (point *B*). Next, moving from *B* towards *C*, the engine speed increases and so does the flywheel, reducing the power gain P_l/P_e ; note that the bigger the flywheel, the slower is the displacement from *B* to *C*. When the ratio i reaches the value of the new target gear ratio τ_{III} , the clutch can be closed very quickly and the vehicle propelled again through the gearbox. In conclusion, the torque gap can be partially filled and the engine keeps on operating at energy efficient points during all the gear shift phase.

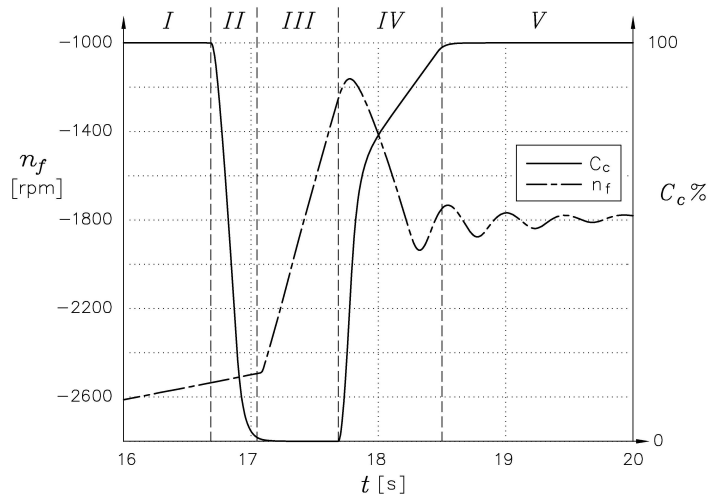


Figure 9: down shift: flywheel angular speed and clutch command (right axis)

3.2 Up shift

A different behaviour takes place during an up shift phase, when different strategies can be actuated to control the engine and flywheel dynamics depending on the desired target of the modified transmission: comfort, driveability, acceleration or fuel saving. Among the different scenarios the authors propose a control that maximize the power transferred to the wheels: starting from point A' correspondent to a low gear (i.e. $\tau_{II} > i^*$) the flywheel has a positive speed and, due to the engine torque, it moves towards B' , thus absorbing energy. When the clutch is closed, B' jumps to C' because the clutch forces the flywheel to recover the kinematic equilibrium of the planetary set ($\dot{\omega}_f < 0$): during the slipping phase up to point D' , the flywheel transfers power to the wheels. Part of the total available energy is dissipated by friction in the clutch itself. It must be noted that, in order to follow the proposed model, it could be necessary to increase the maximum value of the torque transmitted by the clutch.

Another choice, in order to minimize the clutch slip, may be to release the accelerator aiming at reducing the engine speed so that it can quickly match the value correspondent to the new gear ratio (τ_{III}), moving from C'' to D' . The slip time is drastically reduced, but the engine braking power is transferred to the vehicle thus amplifying the output torque gap.

4 Numerical simulations

The proposed driveline layout is tested numerically on a complete vehicle model and the results are compared with those obtained mounting a classical MT system.

In particular the following manoeuvres are tested:

- down shift with $\tau < i^*$, starting with high vehicle speed and high gear, at constant throttle valve opening (TVO) and road slope 20%;
- sequence of up shifts from τ_I to τ_{IV} , accelerating the vehicle from low gear and low speed, at constant TVO on a flat road.

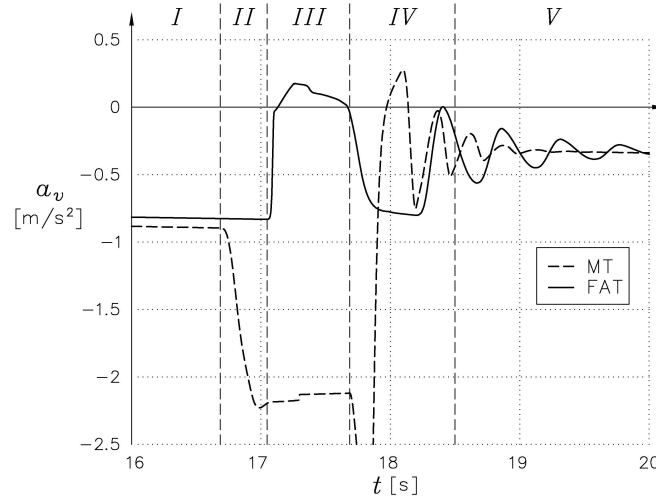


Figure 10: down shift: vehicle acceleration

The driver control logic acts a gear shift when the engine speed falls under 1500 rpm or when it reaches 5000 rpm. The clutch opening profile is the same for FAT and MT; the accelerator command is constant for the FAT while for MT it is released during the gear shift like the driver of a manual transmission would do. The overall duration of the gear shift phase is about 2 seconds. The manoeuvres start with the same vehicle speed and gear for both the tested transmissions. The vehicle tested is a middle sedan (see data in Tab. A in Appendix A); the flywheel inertia $J_f = 0.5 \text{ kgm}^2$, $\beta_s = 1.3$ and $i^* = 1.84$, chosen between τ_{II} and τ_{III} , represent a good compromise between the increased performance during the gear shifts and the reduced acceleration with gear engaged (see Fig. 7 and 8).

An example of the vehicles behaviour during a down shift manoeuvre from τ_V to τ_{IV} is shown in Figs. 9 and 10. Fig. 9 plots the flywheel angular speed and the clutch command (conventionally the

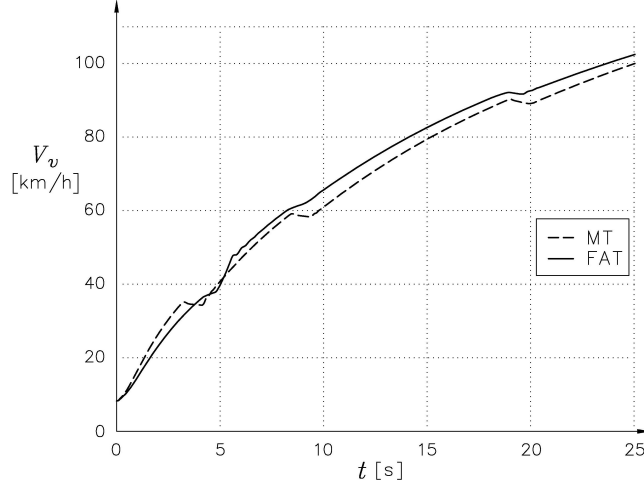


Figure 11: up shift: vehicle speed

clutch command is 100% when the clutch is completely engaged and 0% when disengaged). Fig. 10 displays the accelerations for the two transmissions: the manual transmission is characterized by the typical torque gap, the flywheel assisted system guarantees a smoother transition to the next acceleration, without reducing its mean value, thus improving the comfort during the gear change process [Sorniotti et al. (2007)]. In region *I* the acceleration of the FA vehicle is larger because the flywheel has a positive effect on the dynamics since it is delivering part of the stored kinetic energy to the load shaft. In zone *II* the clutch opens: while the MT vehicle reduces its acceleration due to the pedal release, the FA shows a constant value because a constant TVO value is imposed. In region *III* the clutch is disengaged: the MT load shaft is completely disconnected from the engine; conversely the flywheel deceleration assures the continuity of the power transmission to the wheels, as visible in Fig. 10. Moreover the acceleration is higher than in region *V* because the torque ratio β_s is larger than τ_{IV} and the engine is delivering approximatively the same torque; the duration of this phase is prolonged beyond the kinematic condition correspondent to the following gear ratio. In zone *IV* the clutch is re-engaged: during the slipping phase the flywheel absorbs part of the engine power thus increasing the modulus of its speed, while the engine slows down and part of the torque progressively flows to the wheels through the gearbox. The vehicle acceleration is reduced, with respect to phase *III*, because the torque acting on the load shaft is decreased by the intervention of the clutch, passing from $\beta_s T_e$ to $\beta_s T_e - (\beta_s - \tau_{IV}) T_{cl}$.

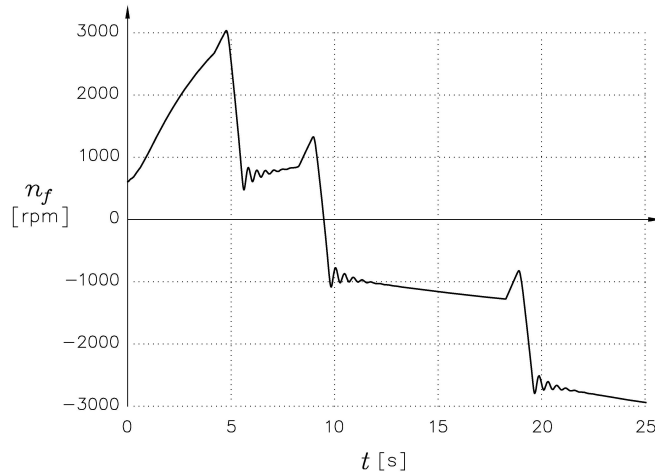


Figure 12: up shift: flywheel speed

Figures 11 and 12 refer to the vehicle acceleration from low speed (10 km/h) up to 100 km/h

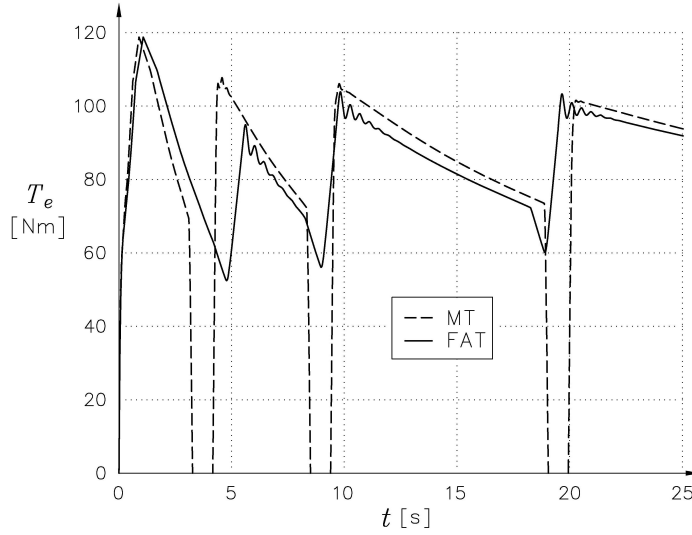


Figure 13: up shift: engine torques

with constant $TVO = 70\%$, showing a sequence of up shifts (from *I* to *IV*). Obviously in the fixed gear run the additional inertia of the FA equipment is unfavourable: this is clearly visible, for example, in the first part of the plot in Fig. 11; conversely during the gear shift phases, the continuity of the connection between the engine and the wheels assure a better performance. In the considered test, the FA vehicle reaches the target speed approximatively 1.7 s in advance. Finally, the flywheel speed versus time is plotted in Fig. 12: initially the flywheel stores energy increasing its positive speed and suddenly releasing it during the gear shift. This behaviour changes when τ is greater than i^* : when this situation occurs the flywheel speed changes its sign. Moreover at high gears the energy delivered during the gear shift is significantly reduced in comparison with the former situation.

In Fig. 13 the engine torques are shown: while in the MT case the torque falls when the accelerator pedal is released during the gear shift, in the FA case the engine is subject to a continuous load due to the flywheel, thus operating in better efficiency conditions and partially filling the torque gap.

5 Conclusions

In the paper the authors presented the model of a flywheel assisted driveline to be used in vehicles equipped with AMT. The passive device is constituted by an epicyclic gearing mounted between the engine shaft and the gearbox output shaft, connected also with a flywheel, with the aim of reducing the torque gap occurring during the gear shifts.

The model of the systems in the different dynamic conditions of the clutch (engaged, sliding and disengaged) proves that it can guarantee a better dynamic behaviour during the gear shifts, reducing the torque gap and enhancing the vehicle acceleration during the transient.

The proposed transmission model could be further improved by inserting one or more clutch in order to engage or disengage the additional flywheel depending on the dynamics, thus realizing an active assisted system, that could optimize the vehicle performances.

References

- K. Koprubasi, E. Westervelt, G. Rizzoni, E. Galvagno, M. Velardocchia, Experimental Validation of a Model for Control of Drivability in a Hybrid-Electric Vehicle, ASME Int. Mechanical Engineering Cong., Seattle, 2007
- M. Kulkarni, T. Shim, Y. Zhang, Shift dynamics and control of dual-clutch transmissions, Mechanism and Machine Theory 42, 2007, pp.168–182
- H. Kuroiwa, N. Ozaki, T. Okada, M. Yamasaki, Next-generation Fuel-efficient Automated Manual Transmission, Hitachi Review, 53, 4, 2004, pp.205–209

- D.H. Park, T.S. Seo, D.G. Lim, H.B. Cho, Theoretical Investigation on Automatic Transmission Efficiency, Electronic Transmission Controls, SAE 960426, 2000
- A.F.A. Serrarens, S. Shen, F.E. Veldpaus, Control of a Flywheel Assisted Driveline With Continuously Variable Transmission, Journal of Dynamic Systems, Measurement, and Control 125, 3, 2003, pp. 455–461
- A. Sorniotti, E. Galvagno, A. Morgando, M. Velardocchia, F. Amisano, An Objective Evaluation of the Comfort during the Gear Change Process, SAE Int. Cong., Detroit, 2007-01-1584, 2007
- R.M. van Druten, Transmission Design of the Zero Inertia Powertrain, Ph.D. thesis, Technische Universiteit Eindhoven, The Netherlands, 2001
- B. Vroemen, A. Serrarens, M. Pesgens, R. van Druten, Performance Analysis of the Impulse Shift CVT, Int. Continuously Variable and Hybrid Transmission Cong., Eindhoven, The Netherlands, 2004

A Appendix A

m	=	1200	kg	τ_I	=	3.9	i_1	=	3.5
R	=	0.3	m	τ_{II}	=	2.2	i_2	=	0.4
J_1	=	0.25	kgm ²	τ_{III}	=	1.4	σ	=	4
F_0	=	114	N	τ_{IV}	=	1.0	δ_{dw}	=	20%
F_2	=	0.45	Ns ² /m ²	τ_V	=	0.7	δ_{up}	=	0%
k_f	=	$3 \cdot 10^{-4}$	Nms ²	τ_f	=	3.5	T_{cl}	=	400 Nm
J_f	=	0.5	kgm ²	i^*	=	1.8	$T_{e,\max}$	=	180 Nm
γ	=	0.72		β_S	=	1.33	$P_{e,\max}$	=	51 kW

Table 1: Vehicle data